Towards Verified and Validated FE Simulations of a Femur with a Cemented Hip Prosthesis

Zohar Yosibash[a,*], Alon Katz[a], Charles Milgrom[b]

[a]*Department of Mechanical Engineering, Ben-Gurion University, Beer-Sheva, Israel*
[b]*Department of Orthopaedics, Hadassah University Hospital, Jerusalem, Israel*

Abstract

Background: Verified and validated CT-based high-order finite element (FE) methods were developed that predict accurately the mechanical response of patient-specific *intact* femurs. Here we extend these capabilities to human femurs undergoing a total hip replacement using cemented prostheses.

Methods: A fresh-frozen human femur was CT-scanned and thereafter in-vitro loaded in a stance position until fracture at the neck. The head and neck were removed and the femur was implanted with a cemented prosthesis. The fixed femur was CT-scanned and loaded through the prosthesis so that strains and displacements were measured. High-order FE models based on the CT scans, mimicking the experiments, were constructed to check the simulations prediction capabilities.

Results: The FE models were verified and results were compared to the experimental observations. The correlation between the experimental and FE strains and displacements were ($R^2 = 0.97$, $EXP = 0.96FE + 0.02$) for the intact femur and ($R^2 = 0.90$, $EXP = 0.946FE + 0.0012$) for the implanted femur. This is considered a good agreement considering the uncertainties encountered by the heavy distortion embedded in the CT scan of the metallic prosthesis .

Discussion: The patient-specific FE model of the fresh-frozen femur with the cemented metallic prosthesis showed a good correlation to experimental observations, both when con-

*Corresponding author
Email address: zohary@bgu.ac.il (Zohar Yosibash)

sidering surface strains, displacements and strains on the prosthesis. The relatively short timescale to generate and analyze such femurs (about six hours) make these analyses a very attractive tool to be used in clinical practice for optimization prostheses (dimensions, location and configuration), and allow to quantify the stress shielding.
Keywords: THA, p-FEMs, femur

1. Introduction

The mechanical response of a femur fixed by metal devices has been of major interest in the past decade. As of today, the main tools available to surgeons in decision making regarding fixation devices/methods are case reports and meta-analyses. Due to the presence of a fracture and a metal fixation device, stress distribution may change and cause *stress shielding*[1] ; thus the outcome of the fixation depends upon the chosen fixation device and type of fracture [1].

Using the current methods of hip fixations, typically an aggressive approach (surgical intervention) is undertaken to repair hip fractures to restore mobility, especially with ambulatory patients. One of the most common methods of treatment is a total hip arthroplasty (THA), where the femoral head and neck are surgically removed and the intramedullary cavity is expanded to allow the insertion of a metallic prosthetic [2]. In 2005, in the USA alone, the number of hospital admissions for all hip fractures reached 350,000 with more than 280,000 THA procedures [3].

To increase life span and functionality of fixation devices, a large number of studies suggest the use of finite elements analysis (FEA). Among the different examined parameters are: change in stress distribution in the fracture region [4], maximum stresses on the fixation device [5], the ability of different devices to stabilize different fractures [6, 7], and micro motion in the bone prosthesis interface [8].

In order to use the conclusions of these studies for clinical practice, one must perform a

[1]Changes of stress distribution (due to the presence of a fixation device) leads to changes in bone's tissue density and increase risk of prosthesis loosening.

mathematical *verification* and experimental *validation* (V&V) of the numerical model [9, 10]. Fresh-frozen femurs used in in-vitro experiments are mostly recommended for validation purposes, however, due to difficulties encountered in such experiments, replacements for fresh-frozen femurs are often considered (or validation by experimental observation is not done at all [4, 5, 7]). Among the common replacements are: standardized synthetic femurs [11, 12] and dry human bones [13]. However, there is no consensus as to whether synthetic femurs represent the mechanical response at the bone-metal interface [14, 15], and dry bones are known to have different material properties than fresh frozen bones [16]. The use of bones which are not proven to simulate in-vivo bones may lead to false conclusions. Seven intact cadaveric femurs implanted with cementless femoral stems have been recently investigated by conventional FE methods, and the "von-Mises" strains were compared to these measured in in-vitro tests under a stance position loading. A good correlation is reported between the FE von-Mises strains and these measured in the experiments [17]. In the reported study the FE results are not verified (there is no report on the error associated with the numerical results), the FE models of the implanted femurs are constructed without having the exact position of the prosthesis within the femur, and a somewhat artificial measure (von-Mises strains) is used as the basis of comparison between the FE and experimental results.

To the best of the authors' knowledge, a study which verify and validate the numerical model of a fractured fresh-frozen human femur fixed by a cemented prosthesis is not available yet, except for a pioneering study performed three decades ago with limited finite element methodology available at the time [18]. The objective of this study is to determine whether the verified and validated high-order FE modeling of intact femurs [19, 20, 21, 22] can be extended to a femur implanted with a cemented prosthesis that may distort the CT-scan. A detailed algorithm for the construction of patient-specific FE models of femurs from CT-scans (without and with a prosthesis) followed by experimental validation on a fresh frozen human femur is presented.

2. Materials and Methods

A fresh-frozen intact human femur was loaded at a stance position. To validate the numerical predictions, strain at 13 locations and displacements at 2 locations were recorded. Following the set of experiments, the bone was loaded to fracture which occurred at the femoral neck. Later the bone was stabilized by a cemented prosthesis and loaded again (see Figure 1). The femur was CT-scanned both in its intact state and after the prosthesis was inserted.

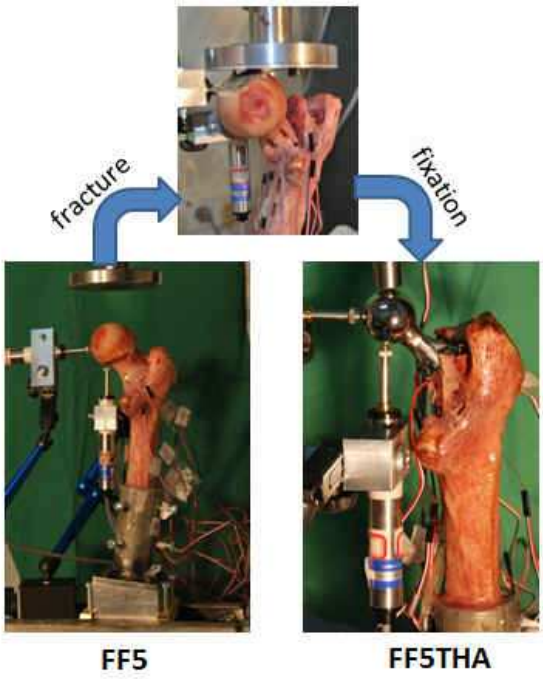

Figure 1: Experimental diagram

2.1. In-vitro Experiments

2.1.1. The Specimen

A right femur of a 56-year-old male donor, deceased due to myocardial infarction with no skeletal disease or lesions, was used for this study. To minimize the alteration of the mechanical properties of the bone tissues, the bone was harvested and kept deep-frozen. On the day of experiment, the bone was thawed at room temperature; soft tissue was removed from the bone by a combination of sharp and blunt dissection. The bone was degreased

with ethanol, and at sites at which strain-gauges (SGs) were to be applied, the bone was roughened with 400 grit sandpaper. The femur was then cut to 170mm and mounted into a cylindrical steel device. The mounting jig is documented in [19].

Prior to bonding the strain gauges, the bone was QCT scanned in water by a Phillips Brilliance 64 scanner (Eindhoven, Netherlands): 120 kVp, 1.25 mm slice thickness, axial scan without overlap, and voxel size of 0.26mm. For calibration, five burettes were immersed in the water near the femur, containing the following concentrations of K_2HPO_4: $[0, 50, 100, 200, 300]\,\mathrm{mg/cm^3}$ [23].

Thirteen uniaxial strain gauges were serially bonded to the superior and inferior neck and the medial and lateral shaft, using M-Bond 200 Cyanoacrylate Adhesive (Measurements Group, Inc., Raleigh, NC, USA) (see SG distribution in Fig 2). The SGs were bonded to align with the assumed local principal strain directions (E_1 or E_3).

Four hours following the QCT scan, mechanical experiments were started, and lasted nearly 24 hours. During bone preparation and between tests the bone was hydrated and stored in a cold humid container and refrigerated overnight.

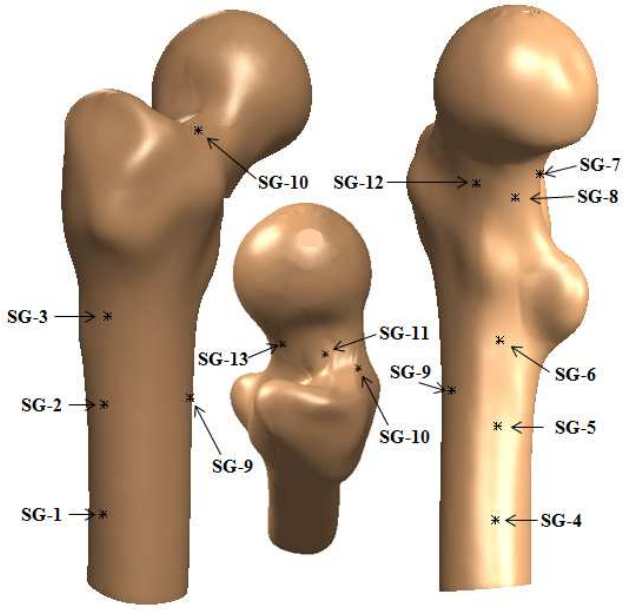

Figure 2: FF5: SGs bonded on the femur.

2.1.2. In-vitro Experiments on the Intact and Fractured Femur with a Prosthesis

A load was applied to the head of the femur, in the shaft direction, at 3 discrete inclination angles of the shaft: 0°, 7° and 15°. A screw driven loading machine Zwick 1445 (Zwick Gmbh & Co. KG., Germany 1992) was used for all tests. Nominal load range of the load cell is $\pm 10kN$ (precision of $\pm 0.5\%$). A flat and smooth aluminum plate applied load directly to femur's head. Vishay general purpose uniaxial strain gauges (SG) were used to measure strains (sensitivity of $\pm 0.2\%$). Vishay linear displacement sensors (LDS, precision of $\pm 0.2\%$) were used to measure displacements at two locations. Vishay system 7000 combined with Strain-Smart software was used to record the output data from the load cell (via an amplifier), SGs and LDS.

To confirm repeatability, six loading-unloading cycles were performed. First time loading to 500 N and unloading, then five consecutive loading to 1000N and unloading. The effect of loading rates $[\frac{1}{60} : 1] \left[\frac{mm}{sec}\right]$ on the mechanical response was shown to be marginal [24], thus the loading rate of $\frac{1}{2} \left[\frac{mm}{sec}\right]$ was used. Vertical U_z (load direction) and horizontal U_y displacements of the femoral head were measured.

Following these experiments, the femur named FF5 was loaded at 15° to failure, which was obtained at approximately 10,000 N (see Figure 3). The femur was then stored in a cooled and humid container and the neck fracture was stabilized by three titanium screws ($\phi_{outer} = 5\,mm$, $\phi_{inner} = 3.45\,mm$ $L = 90, 95, 100\,mm$). The fixed femur was loaded on its head to fracture which resulted in severe damage to the head and neck. The entire procedure lasted 14 hours. The femur was then deep-frozen ($-70°$ C) for four weeks after which the head and neck were removed and a THA prosthesis (Zimmer USA, Warsaw, Indiana, 46580, Versys Heritage, size 10, composed of Co-Cr-Mo) was implanted to the femur by bone-cement (according to manufacturer procedures [25]). The prosthesis was implanted into the femur by an experienced orthopaedic surgeon.

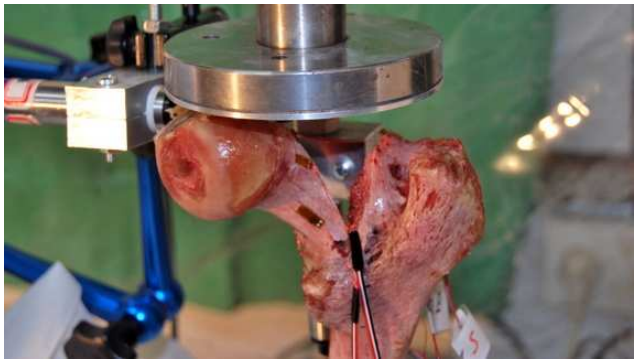

Figure 3: FF5: load to fracture.

The femur with the prosthesis is denoted by FF5THA. Six of the 13 SGs bonded to FF5 were damaged during bone fracture, transportation and fixation. The remaining functioning SGs were: 1-6, and 9 (for SGs positioning see Figure 2). To validate strain predictions on the prosthesis, four SGs were bonded to it (see Figure 4). Same experiments performed on FF5 were re-performed on FF5THA.

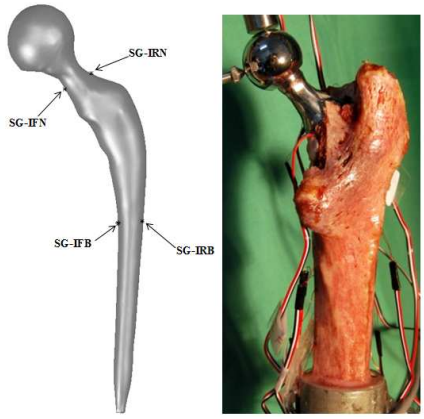

Figure 4: FF5THA: SG positions on prosthesis

2.2. p-FE Models

The QCT-scans are being manipulated by automatical methods, detailed in [20, 21], resulting in a high-order finite-element mesh. In this work technical and algorithmic improvements were incorporated that reduce the geometric construction of the patient-specific femur's model to approximately two hours and the solution time (a series of linear elastic

p-FE solutions are performed by increasing the polynomial degree over the elements until convergence is achieved) to approximately two hours also. Key dimensions of the geometric model generated from the QCT-scan were checked by measurements on the actual femur, shown to be accurate to at most 2% relative error. In Figure 5 the accuracy of the geometrical model is illustrated, as well as the FE mesh used for the intact bone and boundary conditions that mimic the experiments.

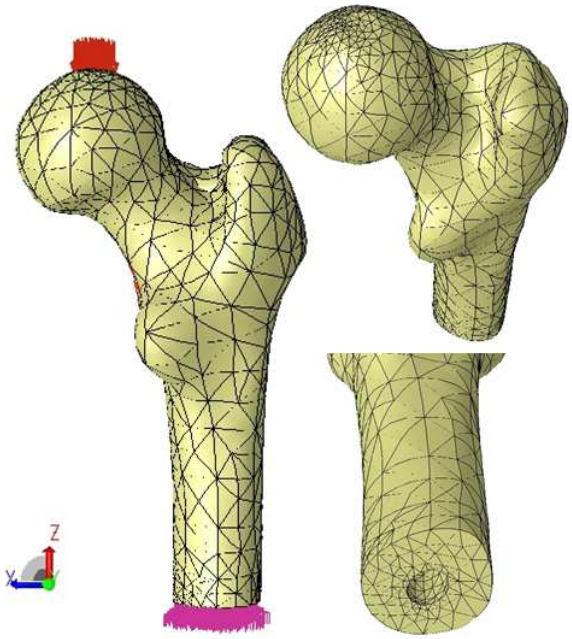

(a) FF5: mesh refinement and BC configuration.

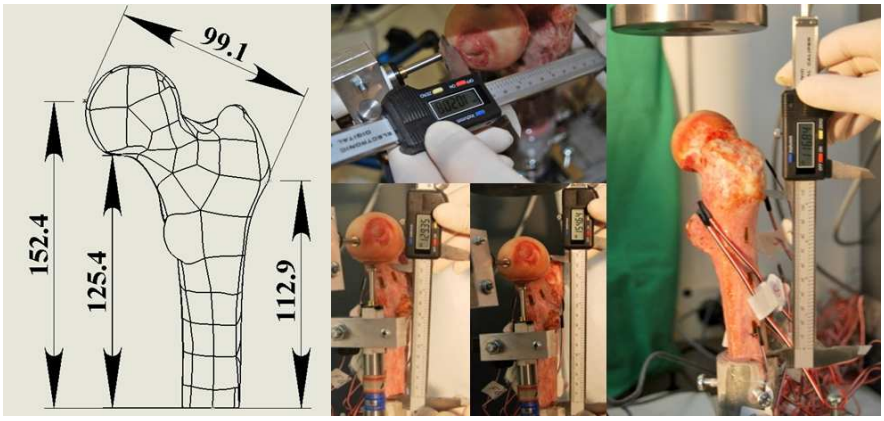

(b) FF5: Geometrical deviation.

Figure 5: FF5: p-FE model

In the QCT-scan of the femur with the prosthesis, due to the alloy composition of the prosthesis, the images were corrupted, affecting the voxel density values, therefore the material property and the bone geometry were affected. To overcome the artifacts in the QCT-scan, the bone model from the QCT-scan of the intact bone was used instead. The model

construction algorithm is illustrated in Fig 6.

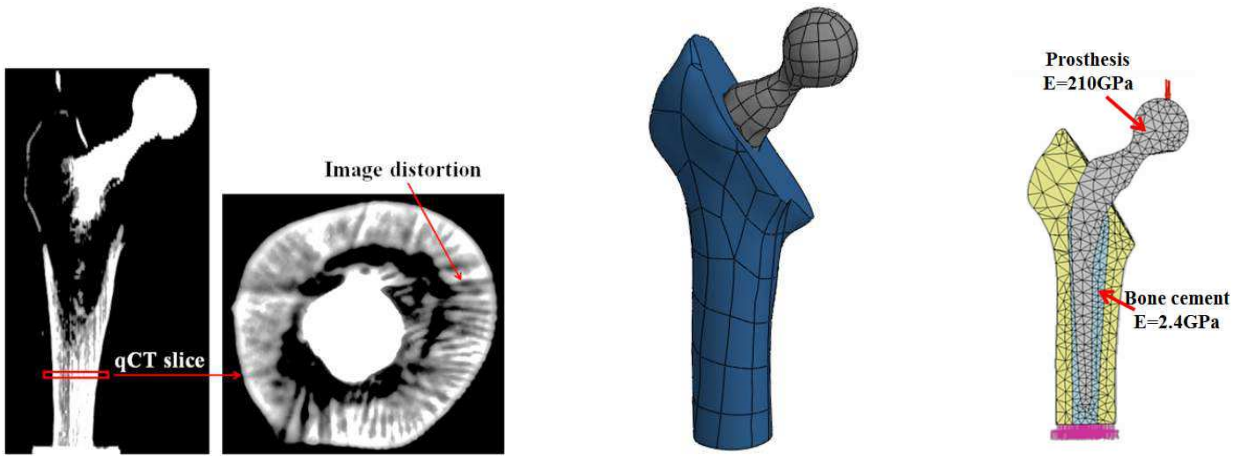

(a) (b) (c)

(a) Image of the distorted QCT of FF5THA.

(b) Only the geometry of the prosthesis was reconstructed from the distorted QCT and positioned within the bone reconstructed from the undistorted QCT performed on FF5. The bone was cut to the shape of FF5THA in the neck region. The bone's intramedullary cavity (filled by bone cement) was manually expanded to surround the entire prosthesis.

(c) The solid models of the bone, prosthesis and cavity were imported to the FE code and meshed by an automatic mesh-generator.

Figure 6: FF5THA: FE model generation.

FF5THA included approximately 7500 high-order tetrahedral elements. All interfaces were modeled as completely bonded i.e. bone/bone-cement, bone-cement/prosthesis. The model was fully constrained at the distal part of the shaft and small loading surfaces were created on the head of the prosthesis.

2.2.1. Assigning Inhomogeneous Material Properties to the Femur

Under a simplified "stance position" loading, an inhomogeneous isotropic material model in FE simulations provides very good results for the intact femur when compared to experimental observation [26, 21, 27, 22, 28]. Many empirical material models that correlates the Young's modulus to a densitometric measure are available in the literature (see the survey

[29]). In [20, 21, 22] we found that p-FE analyses with the relationships in [30] (the cortical connections are based on [31]) provide the closest results to in-vitro experiments on the proximal femur:

$$\rho_{EQM} = 10^{-3}\left(a \times HU - b\right) \quad [g/cm^3] \tag{1}$$

$$\rho_{ash} = \left(1.22 \times \rho_{EQM} + 0.0523\right) \quad [g/cm^3] \tag{2}$$

$$E_{Cort} = 10200 \times \rho_{ash}^{2.01} \quad [MPa] \quad \rho_{ash} > 0.6 \tag{3}$$

$$E_{Trab} = 5307 \times \rho_{ash} + 469 \quad [MPa] \quad 0.27 < \rho_{ash} \leq 0.6 \tag{4}$$

$$E_{Trab} = 33900 \times \rho_{ash}^{2.20} \quad [MPa] \quad \rho_{ash} \leq 0.27 \tag{5}$$

where ρ_{EQM} is the equivalent mineral density, ρ_{ash} is the ash density, E_{Cort}, E_{Trab} are the Young's modulii in the cortical and trabecular regions and the parameters a and b are determined by the K_2HPO_4 phantoms in the CT-scan. Constant Poisson ratio $\nu = 0.3$ was assigned to the entire bone. According to a sensitivity analysis in [19, 20] the influence of ν on the results is very small.

The prosthesis and bone-cement are isotropic homogeneous material with a Poisson ratio of 0.3 and $E_{prosthesis} = 210$ GPa, $E_{cement} = 2.4$ GPa.

2.2.2. Verification of p-FE Results and Comparison Between Simulation and Experimental Results

p-FE results are being verified so to ensure that the numerical error is under a specific tolerance. Convergence is realized by keeping a fixed mesh (with relatively large elements) and increasing the polynomial degree of the approximated solution p. To this end, the polynomial degree over the elements is increased until the relative error in energy norm is small, and the strains at the points of interest converge to a given value. Such verifications are presented in the results section.

To determine the accuracy and reliability of the p-FE results, after the verification process the numerical strains and displacements are compared to the experimental data, i.e. linear regression analyses are performed and presented for each model. Measured values are treated as the independent variables, and the predicted values were the dependent ones.

For each FE analysis the strains at the location of the strain-gauges (SGs) were averaged over a small area representing the area over which the SG measured the strains. Because uni-axial SGs were used in our experiments, we considered the FE-strain component in the direction coinciding with the SG direction (in most cases the SGs are aligned along the principal strain directions).

If the FE strain along a given orientation (for a given SG location) show a high sensitivity to small changes in the orientation, then these strains are not considered for the validation process (this occurred for two SGs only as will be discussed in the next section).

2.2.3. Stress (Strain) Shielding

It is well known in the clinical community that if the stress-distribution in the femur is changed, a remodeling occurs so that the bone density (and a consequence bone's quality) changes in the vicinity of the cemented prosthesis, which may lead to loosening and eventually to the need for a re-operation. The "stress-shielding" terminology is often used, referring to the stress intensification or deterioration in the femur because of the implant.

Comparing the SG data from the experiment to evaluate the stress-shielding effect is a false approach for two reasons: a) Although the load on the femur's head and prosthesis' head is the same loading, the moment along the femur that this load applies is different because of the different distance of the original femur's head and prosthesis' head. b) The bone tissue closest to the cement is the one of interest (where no SG can be bonded), and the outer surface of the femur on which SGs are boned may experience a different stress/strain change. Therefore, since we have shown that the FE results predict well the measured data, we perform a FE analysis of the implanted femur, at 0° inclination angle with the load being applied to the prosthesis exactly as it is applied to the intact femur (through the pelvis acetabulum), as shown in Figure 7.

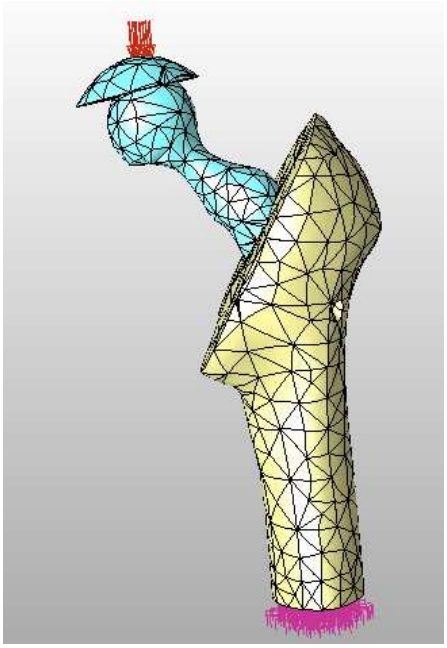

Figure 7: FF5THA with load applied exactly as on the intact femur.

Considering two paths close to the cement-femur interface (in tension and compression) we may extract the principal maximum and minimum strains along the path in the intact and implanted configuration and plot them together. The change in these strains along these paths may indicate whether a pronounced strain (stress) shielding effect is evident.

3. Results

3.1. Experimental results

A linear response between force and strains/displacements was observed in all test results $R^2 > 0.998$. In all five loading circles a good repeatability in the entire measurement range was observed (the largest measured relative deviation in SG measurement was 6.5% in SG-7). Thus, the average results for each inclination angle was computed based on the fourth loading cycle at the measurement close to 1000 N i.e. $\frac{\epsilon(F(1000))[\mu strain]}{F(1000)[N]}$, $\frac{U(F(1000))[\mu m]}{F(1000)[N]}$. Due to technical difficulties at 15° inclination test the LDS that measures U_z could not had been positioned properly, therefore this measurement is absent.

On the intact femur FF5 eleven of the thirteen bonded strain-gauges provided data which was useful. SG-13 was not aligned along the local principal strain E_1. Therefore a local axis system was aligned in the FE-extraction phase with the direction of the SG yet the results showed high sensitivity to slight change in the orientation of the axis system, which could not be determined accurately. SG-11 data was considerably off, possibly due to poor bonding. The total number of measurements (strains and displacements for the three different inclination angles) used for validation was $n = 38$ (given in Table 1).

Table 1: FF5: experimental results $\frac{displacement}{Force}$, $\frac{strain}{Force}$.

Incli-	$(\mu m/N)$		$(\mu strain/N)$										
nation	U_y	U_z	SG_1	SG_2	SG_3	SG_4	SG_5	SG_6	SG_7	SG_8	SG_9	SG_{10}	SG_{12}
0°	0.796	0.533	0.713	0.722	0.548	-1.043	-0.978	-0.911	-0.483	-0.974	-0.439	0.460	-0.793
7°	0.465	0.492	0.464	0.552	0.458	-0.767	-0.784	-0.780	-0.521	-0.965	-0.323	0.466	-0.783
15°	0.051	-	0.101	0.278	0.295	-0.366	-0.492	-0.573	-0.520	-0.868	-0.188	0.334	-0.725

Six of the thirteen SGs bonded to FF5 were damaged during bone fracture, transportation and fixation. The remaining functioning SGs on FFTHA were: 1, 2, 3, 4, 5, 6, 9. In addition, four additional SGs were bonded to the prosthesis, however one was damaged during the fixation, possibly due to the high temperature during bone-cement solidification. There were a total of ten SGs. The total number of measurements used for FF5THA validation was $n = 35$ (given in Table 2).

Table 2: FF5THA: experimental results $\frac{displacement}{Force}$, $\frac{strain}{Force}$.

Incli-	$(\mu m/N)$		$(\mu strain/N)$									
nation	U_y	U_z	SG_1	SG_2	SG_3	SG_4	SG_5	SG_6	SG_9	IRB	IRN	IFN
0°	0.982	0.550	0.707	0.672	0.356	-1.076	-0.909	-0.523	-0.465	0.199	0.308	-0.350
7°	0.354	0.209	0.170	0.304	0.217	-0.457	-0.511	-0.328	-0.330	0.149	0.222	-0.308
15°	0.135		-0.098	0.131	0.157	-0.150	-0.300	-0.217	-0.180	0.132	0.204	-0.261

3.2. p-FE Results and their Verification

To verify that the FE results are accurate, it is necessary to monitor the relative error in energy norm and ensure that the data of interest (strains and displacements) had converged. These measures are easily obtained by a p-FE analysis since the polynomial degree over the FE mesh is increased (the number of degrees of freedom is increased) by using hierarchical spaces [32]. All analyses converged to less than 5% relative error in the energy norm for all inclination angles (see Figure 8(b)) and all the data of interest converged to less than 1% deviation between $p = 5$ and 6.

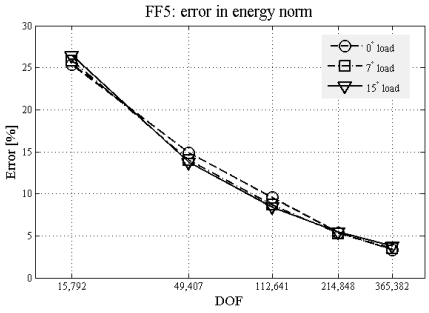

(a) Convergence in energy norm.

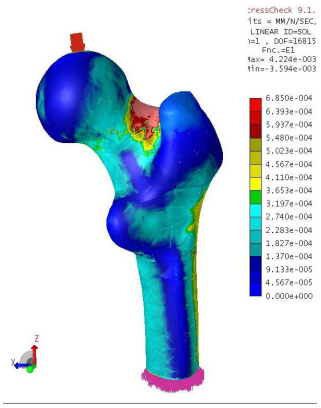

(b) FF5: E_1 at 15° inclination.

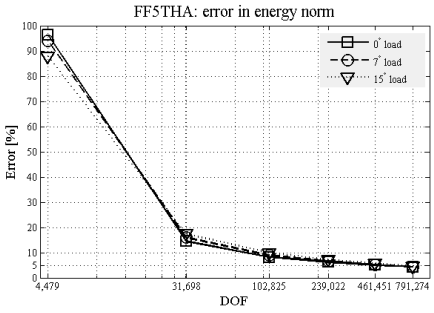

(c) Convergence in energy norm.

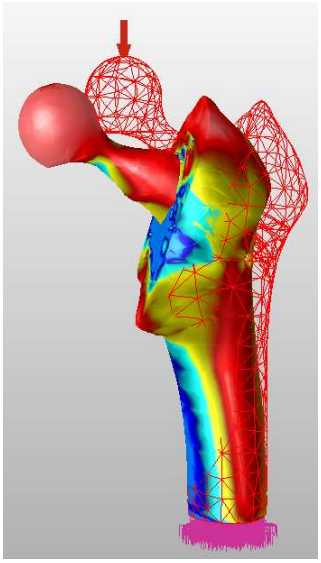

(d) FF5THA: E_1 at 15° inclination.

Figure 8: FF5 and FF5THA mesh and convergence in energy norm.

In Tables 3-4 we summarize the displacements and strains computed by the FE analyses for the FF5 and FF5THA models. The values in parenthesis are the relative errors compared to the experimental values as percentage:

$$\Delta \stackrel{def}{=} 100 \times \frac{EXP - FE}{EXP} \tag{6}$$

Table 3: FF5: FE results and relative error compared to experimental observation.

Incli-	$(\mu m/N)$		$(\mu strain/N)$										
nation	U_y	U_z	SG_1	SG_2	SG_3	SG_4	SG_5	SG_6	SG_7	SG_8	SG_9	SG_{10}	SG_{12}
0°	0.687	0.419	0.807	0.740	0.579	-0.996	-1.011	-1.006	-0.756	-1.012	-0.556	0.607	-1.059
	(14)	(21)	(-14)	(-3)	(-6)	(4)	(-4)	(-11)	(-57)	(-4)	(-27)	(-33)	(-34)
7°	0.459	0.333	0.445	0.454	0.395	-0.632	-0.726	-0.802	-0.615	-0.934	-0.375	0.512	-0.952
	(7)	(29)	(5)	(18)	(14)	(18)	(8)	(-2)	(-17)	(4)	(-15)	(-9)	(-21)
15°	0.183	-	0.102	0.200	0.237	-0.334	-0.410	-0.579	-0.557	-0.797	-0.206	0.376	-0.763
	(-261)	-	(-1)	(28)	(20)	(9)	(17)	(-1)	(-7)	(9)	(-9)	(-12)	(-5)

Table 4: FF5THA: FE results and relative error compared to experimental observation.

Incli-	$(\mu m/N)$		$(\mu strain/N)$									
nation	U_y	U_z	SG_1	SG_2	SG_3	SG_4	SG_5	SG_6	SG_9	IRB	IRN	IFN
0°	0.619	0.258	0.738	0.529	0.575	-0.946	-0.795	-0.798	-0.385	0.299	0.307	-0.409
	(36)	(53)	(-4)	(21)	(-61)	(12)	(12)	(-53)	(17)	(-50)	(0)	(-17)
7°	0.403	0.188	0.399	0.353(	0.438	-0.578	-0.551	-0.619	-0.158	0.229	0.267	-0.367
	(-15)	(10)	(-19)	(-16)	(-102)	(-26)	(-8)	(-89)	(52)	(-53)	(-20)	(-19)
15°	0.102	-	0.034	0.136	0.263	-0.148	-0.258	-0.397	-0.044	0.141	0.211	-0.307
	(24)	-	(135)	(-3)	(-67)	(1)	(14)	(-83)	(75)	(-6)	(-3)	(-18)

3.3. Validation: Comparing Simulated and Experimental Results

The verified FE analyses are used for validation purposes, i.e. to ensure that these indeed represent the biomechanical response of the femur (intact and fractured with the implanted prosthesis). A total of 5 displacements and 33 strains were used to assess the validity of the p-FE simulations for FF5, and 5 displacements and 30 strains for the fractured femur with the prosthesis. In Figures 9 and 10 the pooled FE strains and displacements for FF5 and FF5THA, respectively, are compared to the the experimental observations. This comparison

is demonstrated by two measures: a) A linear regression line where we inspect the slope, intersection and R^2 of the linear regression between the experimental observations and FE predictions, b) A Bland-Altman plot [33], where we compare the error between the experimental observations and FE predictions as a function of the mean value, together with a 95% confidence level (± two standard deviations).

FF5: An excellent correlation is obtained manifested by the following regression parameters

$$Exp = 0.967 \times FE + 0.02, \quad R^2 = 0.97 \tag{7}$$

The average absolute deviation between the experimental measurements and the predicted ones is 20.5%. A large error is introduced by the measurement of U_y at 15°. Neglecting this measurement from the average absolute error of all the measurements reduces the relative error from 20.5% to approximately 15%.

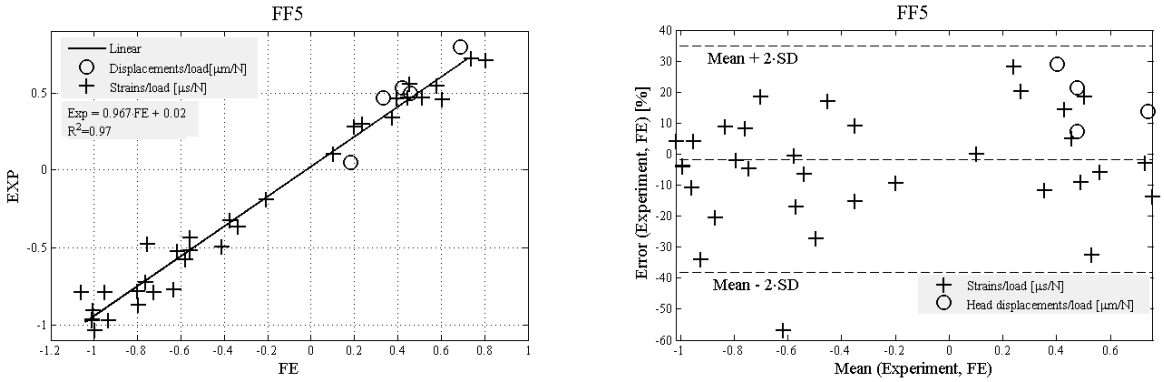

Figure 9: FF5: Left - Linear correlation between FE results and experiments. Right - Bland-Altman plot.

FF5THA: A good correlation is obtained manifested by the following regression parameters

$$Exp = 0.946 \times FE + 0.012, \quad R^2 = 0.90 \tag{8}$$

The mean of the absolute deviations was found to be 31.3%.

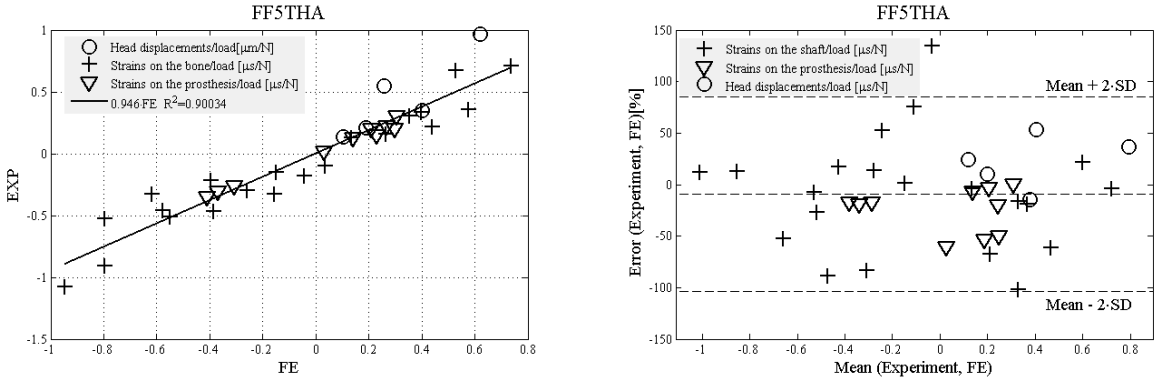

Figure 10: FF5THA: Left - Linear correlation between FE results and experiments. Right - Bland-Altman plot.

We would like to note that the FE results for SGs 11 and 13 experienced high sensitivity to small changes in the orientation in all loading scenarios therefore these measurements were neglected.

3.4. Stress (Strain) Shielding

We consider two paths close to the cement-femur interface (in tension and compression) and extract the principal maximum and minimum strains along them in the intact and implanted configuration and plot them together as shown in Figure 11.

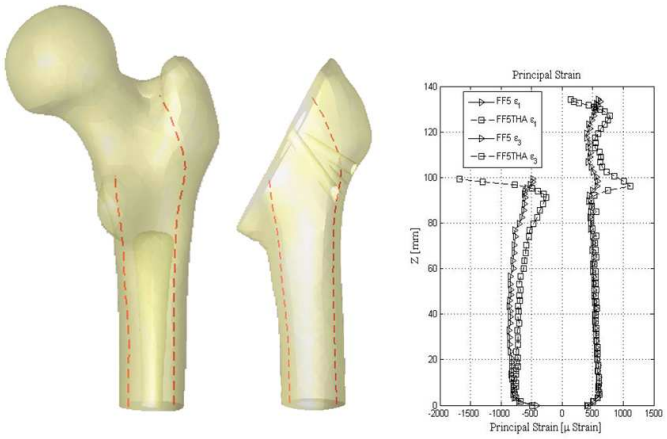

Figure 11: Principal strains at same locations within the intact and fixed femur (principal strains are extracted along the dashed curves in the femur).

The ratio of the principal strains along the path (FF5THA over FF5) may be used as the measure of stress-shielding. This may be one of the criteria for choosing a type and size of the implant.

One may observe that along the shaft the principal strains do not change much, and a large difference is obtained around $Z = 100$ mm. Along the tension path (right path in Figure 11) this difference is attributed to the cylindrical holes of the screws which were left unfilled, and at the compression path, due to the free surface effect. There is also a tensile strain intensification between $135 < Z < 100$, which may be quantified at about 15% increase in principal strains.

4. Discussion

The FE method has been used extensively by many researchers to demonstrate its potential application in orthopedic clinical practice. Many of these FE models fall short of demonstrating that the numerical errors are verified, and thereafter the results match the experimental in-vitro observations, i.e. that the models are validated. A remedy to these two major shortcuts is addressed here in an attempt to analyze a very "popular" orthopedic procedure, the THA with a cemented prosthesis. Since p-FE methods for intact femurs were proven to be verified and double-blinded validated by a large cohort of fresh-frozen femurs [22], with both strains and displacements used as a basis for the validation process; we extend these methods towards their use in clinical practice, for optimizing THA surgery using a cemented prosthesis, for example. To this end we show that the p-FE analyses predict reliably the mechanical response of the femur in-spite of the additional layer of cement and the metallic prosthesis, and may be used to quantify the stress-shielding effect.

The motivation to perform CT-scans, experiments and FE analyses on *both* intact and fractured femur with the prosthesis was two-fold: a) To demonstrate that FE results for both cases are verified and validated, thus can be compared to obtain clinical relevant information on the quality and optimality of the fixation. b) To enable the generation of a reliable FE-model of the femur with the prosthesis since the QCT-scan with the specific alloy of the prosthesis is corrupted.

There are several limitations to the present study: a) Although a large cohort of intact femurs (both genders, large age span, weight and height) have been used to verify and validate (V&V) the p-FE analyses, only one femur with a single type of THA cemented endoprosthesis is used in this study. The promising results of this feasibility study opens the way to many more analyses and in-vitro tests for implanted femurs. b) A single and simplified stance position loading was considered (at three different inclination angles). More realistic loading conditions will be applied in a future study. c) The bone tissue is inhomogeneous orthotropic or transversely isotropic and the application of inhomogeneous isotropic material properties in the FE simulations is a simplification of the reality. For a more complex state of loading, more realistic material properties would probably result in a better correlation with the in-vitro experiments. d) The alloy composition of the prosthesis heavily distort the CT-scan of the femur with the implant, thus the location of the stem in the shaft could not be determined with a very high precision. Most popular and advanced nowadays prostheses are manufactured from titanium that do not cause this distortion. e) Although efforts were made to reduce the friction between the machine punch and prosthesis head, we do not have at this time the ability to measure the friction forces, and cannot determine their influence on the results.

Although there are numerous limitations to our investigation, the correlation between the mean FE results and experimental observations for the intact bone is remarkable (slope= 0.967 and $R^2 = 0.97$ when both strains and displacements are considered), in correspondence with previous works. For the femur implanted by the cemented prosthesis a good correlation is also obtained (slope= 0.946 and $R^2 = 0.90$). Inspecting the Bland-Altman plots, one may notice that the mean difference between the FE and experimental strains and displacements is small and similar for the intact femur and the femur with the cemented prosthesis. However, the scatter in the FE results compared to the experimental observations is considerably larger in the femur with the cemented prosthesis. For a confidence level of 95% (i.e. the relative difference between the FE predictions and the experimental observation is less than $\pm$ two standard deviations), a 100% relative difference should be considered, whereas for the intact femur only 30% should be considered.

We have also shown that such FE analyses can be useful in quantifying the level of strain shielding, and rank possible prostheses according to their best fit in terms of strain and stress shielding consideration. Further quantitative measures should be sought and investigated to determine the best criterion to predict the stress/strain shielding effects to assist the clinical community.

The preliminary encouraging results motivate us to enlarge the number of tested femurs with different cemented prostheses in order to further validate the high-order FE simulations. These may encourage the extension of p-FE simulation to real life orthopedic problems involving metal implants and fixations to the femur.

Conflict of Interest

None of the authors have any conflict of interest to declare that could bias the presented work.

Acknowledgements

We would like to thank Dr. Nir Trabelsi from the Ben-Gurion University of the Negev for his help with FE analyses and experiments. The first author gratefully acknowledges the generous support of the Technical University of Munich - Institute for Advanced Study, funded by the German Excellence Initiative. This study was supported in part by grant no. 3-00000-7375 from the Chief Scientist Office of the Ministry of Health, Israel. Competing interests: None declared. Ethical approval: Not required.

References

[1] L.E. Claes, C.A. Heigele, C. Neidlinger-Wilke, D. Kaspar, W. Seidl, K.J. Margevicius, and P. Augat. Effects of mechanical factors on the fracture healing process. *Clinical Orthopaedics*, 355:132–147, 1998.

[2] I.D. Learmonth, C. Young, and C. Rorabeck. The operation of the century: Total hip replacement. *Lancet*, 370:1508–1519, 2007.

[3] R Iorio, W.J. Robb, W.L. Healy, D.J. Berry, W.J. Hozack, R.F. Kyle, D.G. Lewallen, R.T. Trousdale, W.A. Jiranek, P. Stamos, V, and Parsley B.S. Orthopaedic surgeon workforce and volume assessment for total hip and knee replacement in the united states: preparing for an epidemic. *Jour. Bone Joint Surg.*, 90:1598 – 1605, 2008.

[4] P. Helwig, G. Faust, U. Hindenlang, A. Hirschmuller, L. Konstantinidis, V. Bahrs, N. Sudkamp, and R. Schneider. Finite element analysis of four different implants inserted in different positions to stabilize an idealized trochanteric femoral fracture. *Journal of Care Injured*, 40:288–295, 2009.

[5] C.J. Wang, A.L. Yettram, M.S. Yao, and P. Procter. Finite element analysis of a gamma nail within a fractured femur. *Med. Eng. Phys.*, 20:667–683, 1998.

[6] S. Eberle, C. Gerber, G. von Oldenburg, S. Hungerer, and P. Augat. Type of hip fracture determines load share in intramedullary osteosynthesis. *Clin. Orthop. Rela. Res.*, 467:1972–1980, 2009.

[7] S. Sowmianarayanan, A. Chandrasekaran, and R. Krishna. Finite element analysis of a subtrochanteric fractured femur with dynamic hip screw, dynamic condylar screw, and proximal femur nail implants: A comparative study. *Jour. Eng. Med.*, 222:117–127, 2008.

[8] M.T. Bah, P.B. Nair, M. Taylor, and M. Browne. Efficient computational method for assessing the effects of implant positioning in cementless total hip replacements. *Jour. Biomech.*, 44:1417–1422, 2011.

[9] HB. Henninger, SP. Reese, AE. Anderson, and JA. Weiss. Validation of computational models in biomechanics. *Proc. IMechE, Part H: Engineering in Medicine*, 224(H7):801–812, 2010.

[10] L.E. Schwer. *Guide for verification and validation in computational solid mechanics*. The American Society of Mechanical Engineers (ASME), July 2006.

[11] J. Stolk, N. Verdonschot, L. Cristofolini, A. Toni, and R. Huiskes. Finite element and experimental models of cemented hip joint reconstructions can produce similar bone and cement strains in pre-clinical tests. *Jour. Biomech.*, 35:499–510, 2002.

[12] J. Stolk, D. Janssen, R. Huiskes, and N. Verdonschot. Finite element-based preclinical testing of cemented total hip implants. *Clin. Orthop. Relat. Res.*, 456:138–147, 2007.

[13] D. Simpson, C.J. Brown, A.L. Yettram, P. Procter, and G.J. Andrew. Finite element analysis of intramedullary devices: The effect of the gap between the implant and the finite element analysis of intramedullary devices. *Jour. Eng. Med.*, 222:333–345, 2008.

[14] J. Grant, N. Bishop, N. Gotzen, C. Sprecher, M. Honl, and M. Morlock. Artificial composite bone as a model of human trabecular bone: The implant bone interface. *Jour. Biomech.*, 40:1158–1164, 2007.

[15] R. Zdero, M. Olsen, H. Bougherara, and E.H. Schemitsch. Cancellous bone screw purchase: A comparison of synthetic femurs, human femurs, and finite element analysis. *Eng. Med.*, 222:1175–1183, 2008.

[16] D.T. Reilly and A.H. Burstein. The mechanical properties of cortical bone. *Jour. Bone Joint Surg.*, 56:1001–1022, 1974.

[17] Sune H. Pettersen, Tina S. Wik, and Born Skallerud. Subject specific finite element analysis of stress shielding around a cementless femoral stem. *Clin. Biomech.*, 24:196–202, 2009. 1st Corrigendum, Clin. Biomech., **24**(8), 2009, p. 697. 2nd Corrigendum, Clin. Biomech., **26**(4), 2011, p. 429.

[18] A. Rohlmann, U. Mössner, and G. Bergmann. Finite-element-analysis and experimental investigation in a femur with hip endoprosthesis. *Jour. Biomech.*, 16(9):727–742, 1983.

[19] Z. Yosibash, R. Padan, L. Joscowicz, and C. Milgrom. A CT-based high-order finite element analysis of the human proximal femur compared to in-vitro experiments. *ASME Jour. Biomech. Eng.*, 129(3):297–309, 2007.

[20] Z. Yosibash, N. Trabelsi, and C. Milgrom. Reliable simulations of the human proximal femur by high-order finite element analysis validated by experimental observations. *Jour. Biomech.*, 40:3688–3699, 2007.

[21] N. Trabelsi, Z. Yosibash, and C. Milgrom. Validation of subject-specific automated p-FE analysis of the proximal femur. *Jour. Biomech.*, 42:234–241, 2009.

[22] N. Trabelsi, Z. Yosibash, C. Wutte, R. Augat, and S. Eberle. Patient-specific finite element analysis of the human femur - a double-blinded biomechanical validation. *Jour. Biomech.*, 44:1666 – 1672, 2011.

[23] C.E. Cann. Quantitative CT for determination of bone mineral density: A review. *Radiology*, 166:509–522, 1988.

[24] Z. Yosibash, D. Tal, and N. Trabelsi. Predicting the yield of the proximal femur using high order finite element analysis with inhomogeneous orthotropic material properties. *Philosophycal Transaction of the Royal Society: A*, 368:2707–2723, 2010.

[25] D.K. Collis, J.C. Couceiro, R.C. Johnston, and E.A. Slavati. *Surgical technique for VerSys heritage primary hip prosthesis*, 2005.

[26] M. Viceconti, F. Taddei, L. Cristofolini, S. Martel, and H.S. Gillc. Subject-specific finite element models of long bones: An in vitro evaluation of the overall accuracy. *Jour. Biomech.*, 39:2982–2989, 2006.

[27] H. Yang, X. Ma, and T. Guo. Some factors that affect the comparison between isotropic and orthotropic inhomogeneous finite element material models of femur. *Med. Eng. Phys.*, 32:553–560, 2010.

[28] N. Trabelsi and Z. Yosibash. Patient-specific FE analyses of the proximal femur with orthotropic material properties validated by experiments. *ASME Jour. Biomech. Eng.*, 155:061001–1 – 061001–11, 2011.

[29] B. Helgason, E. Perilli, E. Schileo, F. Taddei, S. Brynjolfsson, and M. Viceconti. Mathematical relationships between bone density and mechanical properties: A literature review. *Clin. Biomech.*, 23:135 – 146, 2008.

[30] JH. Keyak and Y. Falkinstein. Comparison of in situ and in vitro CT scan-based finite element model predictions of proximal femoral fracture load. *Med. Eng. Phys.*, 25:781–787, 2003.

[31] T. S. Keller. Predicting the compressive mechanical behavior of bone. *Jour. Biomech.*, 27:1159–1168, 1994.

[32] B. A. Szabó and I. Babuška. *Finite Element Analysis*. John Wiley & Sons, New York, 1991.

[33] JM. Bland and DG. Altman. Statistical methods for assessing agreement between two methods of clinical measurement. *Lancet*, 1(8476):307 – 310, 1986.